Linear and nonlinear dust acoustic waves in an inhomogeneous magnetized dusty plasma with nonextensive electrons

W. F. El-Taibany, M. M. Selim, N. A. El-Bedwehy, and O. M. Al-Abbasy

Citation: Physics of Plasmas (1994-present) **21**, 073710 (2014); doi: 10.1063/1.4890853
View online: http://dx.doi.org/10.1063/1.4890853
View Table of Contents: http://scitation.aip.org/content/aip/journal/pop/21/7?ver=pdfcov
Published by the AIP Publishing

PHYSICS OF PLASMAS 21, 073710 (2014)

Linear and nonlinear dust acoustic waves in an inhomogeneous magnetized dusty plasma with nonextensive electrons

W. F. El-Taibany,[1,a)] M. M. Selim,[1] N. A. El-Bedwehy,[2,b)] and O. M. Al-Abbasy[1]
[1]Department of Physics, Faculty of Science, Damietta University, New Damietta P. O. 34517, Egypt
[2]Department of Mathematics, Faculty of Science, Damietta University, New Damietta P. O. 34517, Egypt

(Received 26 May 2014; accepted 9 July 2014; published online 23 July 2014)

The propagation of both linear and nonlinear dust acoustic waves (DAWs) in an inhomogeneous magnetized collisional and warm dusty plasma (DP) consisting of Boltzmann ions, nonextensive electrons, and inertial dust particles is investigated. The number density gradients of all DP components besides the inhomogeneities of electrostatic potential and the initial dust fluid velocity are taken into account. The linear dispersion relation and a nonlinear modified Zakharov-Kusnetsov (MZK) equation governing the propagation of the three-dimensional DAWs are derived. The analytical solution of the MZK reveals the creation of both compressive and rarefactive DAW solitons in the proposed model. It is found that the inhomogeneity dimension parameter and the electron nonextensive parameter affect significantly the nonlinear DAW's amplitude, width, and Mach number. The relations of our findings with some astrophysical situations have been given.
 [http://dx.doi.org/10.1063/1.4890853]

I. INTRODUCTION

Recently, dusty plasmas (DPs) have received much attention because of their applications in space and astrophysical systems, such as the planetary rings (Saturn's rings), asteroid zones, cometary tails, interstellar clouds, lower parts of the Earth's ionosphere[1–3] and magnetosphere, as well in laboratory environments.[4–7] The presence of high negatively charged and massive grains of dust particles in electron–ion plasma is responsible for the appearance of new types of waves and instabilities. One of these waves is the low frequency dust acoustic wave (DAW). The existence of DAWs in an unmagnetized DP was reported theoretically first by Rao *et al.*[8] and later it was conclusively verified in a laboratory experiment by Barkan *et al.*[5]

Many authors have discussed various aspects of linear and nonlinear wave propagations in DPs. Although most of these analyses assume the plasmas to be homogenous, inhomogeneity exists widely in space and laboratory discharges. The plasma inhomogeneity may stem from density and/or temperature gradient.[9–11] Singh and Rao[12] presented the analysis of linear and nonlinear DAW propagation in inhomogeneous DP model where the inhomogeneity arises from the gradients of the plasma number density. They found that the amplitude of the linear DAWs is inversely proportional to the square root of the equilibrium dust density, $n_{do}^{-1/2}$, while the amplitude of the nonlinear DAWs is proportional to $n_{do}^{-1/4}$. Considering constant n_{do} with spatially nonuniform dust charge, Li *et al.*[13] proved the existence of compressive solitons whose velocities show complicated behaviors. Misra and Chowdhury[14] derived a Zakharov-Kuznetsov equation for DAWs in an inhomogeneous magnetized hot DP where they also proposed a constant n_{do}. A theoretical model for both dust acoustic solitary waves and shocks in an inhomogeneous magnetized hot DP is presented by El-Taibany *et al.*[9] where this model is applied to interpret the ion acceleration mechanisms close to the Moon. Because of considering density inhomogeneity in a quantum dense DP model, new features are revealed, which cannot be observed in the corresponding homogeneous model.[10] Including the inhomogeneity of the equilibrium density of three-component DP species, Singh and Bharuthram[15] have derived a Korteweg-de Vries equation appropriate for describing the propagation of these nonlinear waves in an inhomogeneous model. They found that DAW's amplitude increases by including nonthermal electrons in a DP model. The nonthermal inhomogeneous DP model of El-Taibany *et al.*[9] is revisited by Zhang and Xue[16] where both dust acoustic solitary holes (soliton with a density dip) and positive solitons (soliton with a density hump) are excited and the linear DAWs are also studied. Alinejad and Mamun[17] proved that the amplitude of DAW decreases as the wave propagates in the direction of increasing dust concentration in a strongly coupled DP model. They introduce the inhomogeneity effect through presenting the polarization force in their model. Moreover, El-Taibany[18] has presented a first attempt to study a four-component inhomogeneous DP model. He found two different DAWs with different velocities. Both compressive and rarefactive solitons are possible is such a multi-component DP model, which is applied in polar mesosphere region. On the other side, recent experiments show that in a neon dc glow discharge, the phase velocity of the density perturbations varies considerably along the plasma column.[19]

Another aspect in DP; nonextensive statistic mechanics based on the deviations of Boltzmann–Gibbs–Shannon B-G-S entropic statistics, is recently focused. A suitable nonextensive generalization of the B-G-S entropy for statistical equilibrium was first recognized by Rényi[20] and subsequently proposed by

[a)]Present address: Department of Physics, College of Science for Girls in Abha, King Khalid University, Abha P.O. 960, Kingdom of Saudi Arabia. Electronic addresses: eltaibany@du.edu.eg and eltaibany@hotmail.com
[b)]Electronic address: nab_elbedwehy@yahoo.com

Tsallis.[21] In these studies, the standard additivity of the entropies to the nonlinear and nonextensive case where one particular parameter, the entropic index q, characterizes the degree of nonextensivity of the system, $q = 1$ corresponds to the standard, extensive, B-G-S statistics. For the macroscopic ergodic equilibrium systems, the limit of the Boltzmann–Gibbs statistics to Maxwell distribution is universally valid. However, for systems with long-range interactions, such as plasma and gravitational systems, where the nonequilibrium stationary states exist, the Maxwellian distribution is inadequate for description of such systems. For electrostatic plane wave propagation in a collisionless thermal plasma, the experimental results show that Tsallis velocity distribution is described by a nonextensive q-parameter smaller than unity.[16] The nonextensivity statistics has successfully applied to a number of astrophysical and cosmological scenarios like stellar polytropes,[22] solar neutrino problem,[23] peculiar velocities of galaxy clusters,[24] dark-matter halos,[25] protoneutron stars[26] hadronic matter and quark-gluon plasma,[27] cosmic ray, cosmology, and systems with long-range interactions.[28] For comprehensive review, see the book of Tsallis.[21] Recently, the most evident theoretical and simulation features on the nonextensivity effects have been employed successfully in plasma physics.[29–38] For instance, based on the theoretical framework of the Tsallis statistical mechanics,[21] Tribeche and Merriche[31] have used Sagdeev potential analysis for investigating the effect of nonextensive electrons on DAW propagation in a homogeneous DP model. They have shown for $q < 0(>)0$, the DAW exhibits compression (rarefaction) features. Also, the lower limit of the Mach number for the existence of these DAWs is greater (smaller) than its Maxwellian counterpart in the case of superextensivity (subextensivity). Later, Tribeche and Shukla[32] have calculated the dust charge number residing on the dust grain surface due to the presence of nonextensive electrons in nonextensive DP model. Asaduzzaman *et al*.[33] have found that in a nonuniform DP, the DAW phase speed is decreased due to the polarization force, however its amplitude increases by increasing the dust density number. Employing their results to the downward current region of the aurora, Roy *et al*.[35] have introduced a study for dust acoustic double layers in a homogeneous DP model containing nonextensive electrons and two-temperature thermal ions. Also, Bains *et al*.[36] have studied the effect of nonextensive electrons and ions on the modulational instability of DAW envelopes. It is found that the instability of DAWs is influenced by the plasma species deviation apart from the Maxwellian distribution. On the other side, the effect of external magnetic field on homogeneous DP model is discussed by Ashraf *et al*.[37]

Therefore, the main aims of the present paper are to study the effects of the DP inhomogeneities, nonextensive distributed electrons, external magnetic field, and collision on the propagation of both linear and nonlinear DAWs in an inhomogeneous DP systems. The outline of the paper is as follows, in Sec. II, we write down the basic fluid equations describing the proposed model. In Sec. III, we use the standard normal-mode analysis to study the features of the linear DAWs. In Sec. IV, the modified Zakharov-Kuznetsov (MZK) equation governing the nonlinear DAWs propagation in inhomogeneous DPs is derived using a reductive perturbation method (RPM).[8–10,12–18,39] The analytical solutions of MZK are presented and numerical results are provided, in Sec. V. Section VI is devoted to discussions and conclusions.

II. GOVERNING EQUATIONS

We consider a three-dimensional, inhomogeneous collisional, and warm DP model having number density gradients for its components along x–direction. This DP model consists of inertial dust grain fluids, nonextensive electrons, and Boltzmann ions in the presence of an external static magnetic field $\mathbf{B_0} = B_0\hat{x}$. At equilibrium, the charge neutrality condition reads $\delta n_{i0}(x) = n_{e0}(x) + (\delta - 1)n_{d0}(x)$ where $n_{i0}(x)$ and $n_{e0}(x)$ are the unperturbed ion and electron number densities, respectively, and $\delta = n_{i0}(0)/n_{e0}(0)$. The normalized basic equations describing this model are given by[9,14,16]

$$\frac{\partial \bar{n}_d}{\partial \bar{t}} + \bar{\nabla}.(\bar{n}_d \bar{\mathbf{u}}_d) = 0, \tag{1}$$

$$\frac{\partial \bar{\mathbf{u}}_d}{\partial \bar{t}} + (\bar{\mathbf{u}}_d.\bar{\nabla})\bar{\mathbf{u}}_d + \frac{5}{3}\sigma \bar{n}_d^{-\frac{1}{3}}\bar{\nabla}\bar{n}_d - \bar{\nabla}\bar{\phi} + \bar{\Omega}(\bar{\mathbf{u}}_d \times \hat{x}) + \bar{\Gamma}\bar{\mathbf{u}}_d = 0, \tag{2}$$

$$\bar{\nabla}^2\bar{\phi} = \bar{n}_d + [(\bar{n}_e - \delta\bar{n}_i)/(\delta - 1)], \tag{3}$$

where $\bar{n}_i(\bar{n}_e)\bar{n}_d$ is the ion (electron) dust number density. $\bar{\mathbf{u}}_d$, $\bar{\phi}$, $\bar{\Omega}$ and $\bar{\Gamma}$ are dust fluid velocity, electrostatic potential, dust cyclotron frequency and dust neutral collision frequency, respectively. $\sigma = T_d/(Z_d T_e)$ and $\Omega = eB_0Z_d/(m_d c)$, where T_e, T_d, Z_d, m_d and c are electron temperature, dust temperature, dust charge number, dust mass and the velocity of light, respectively. In Eqs. (1)–(3), the physical parameters (indicated by upper bars) are defined as: $\bar{n}_d = n_d/n_{d0}$, $\bar{n}_{i,e} = n_{i,e}/(Z_d n_{d0})$, $\bar{\mathbf{u}}_d = \mathbf{u}_d/\sqrt{Z_d T_e/m_d}$, $\bar{\phi} = e\phi/T_e$, $\bar{\nabla} = \nabla\lambda_{Dd} = \nabla\sqrt{T_e/(4\pi e^2 Z_d n_{do})}$, $\bar{t} = t\omega_{pd} = t\sqrt{4\pi e^2 Z_d^2 n_{do}/m_d}$, $\bar{\Omega} = \Omega\omega_{pd}$, and $\bar{\Gamma} = \Gamma\omega_{pd}^{-1}$. λ_{Dd} and ω_{pd} are the modified Debye length and the dust plasma frequency, respectively.

The ions density is governed by the Boltzmann distribution whose form is

$$\bar{n}_i(x) = n_{i0}(x)\exp(-s\bar{\phi}), \tag{4}$$

while the electrons are assumed to obey nonextensive distribution,[31,32] which is given by

$$\bar{n}_e(x) = n_{e0}(x)[1 + (q - 1)\bar{\phi}]^{(q+1)/2(q-1)}, \tag{5}$$

where $s = T_e/T_i$ and T_i is ion temperature. Here, if $q < -1$, the nonextensive electron distribution is unnormalizable while for $q \to 1$, Eq. (5) transforms into the electron Maxwell Boltzmann distribution form.

III. LINEAR ANALYSIS

Following the standard normal-mode analysis,[8,16,40] the plasma parameters appearing in Eqs. (1)–(5) are expanded as:

$$\bar{Q} = Q_0(x) + \bar{Q}_1(x,t), \tag{6}$$

where $\bar{Q} = [\bar{n}_d, \bar{u}_{dx}, \bar{u}_{dy}, \bar{u}_{dz}, \bar{\phi}]$ and $Q_0 = [n_d, 0, 0, 0, 0]$. The perturbed quantities, $\bar{Q}_1(x,t)$, are proportional to $\exp[i(k_x x + k_y y + k_z z - \omega t)]$, where k and ω are the wave number and the frequency, respectively. Substituting Eq. (6) into Eqs. (1)–(5), we finally get the following equation:

$$k^2 + B + \frac{1}{\delta - 1}\left[\frac{q+1}{2} n_{e0}(x) + \delta s n_{i0}(x)\right] = 0, \tag{7}$$

where $B = b_1/(i\omega\gamma A + b_1\alpha)$, $b_1 = k_x A\left[i\frac{\partial n_{d0}(x)}{\partial x} - k_x n_{d0}(x)\right] - (k^2 - k_x^2) n_{d0}(x)\gamma^2$, $\gamma = \Gamma - i\omega$, $A = \gamma^2 + \Omega^2$, and $\alpha = \frac{5}{3}\sigma n_{d0}^{-1/3}$.

Equation (7) is the linear dispersion relation for low frequency DAWs propagating in collisional, magnetized, inhomogeneous DP model including nonextensive electrons. This equation agrees exactly with that derived by Zhang and Xue[16] by ignoring the nonthermal effects of electron/ion species. It is clear that Eq. (7) depends on the DP species inhomogeneities, the collision, the external magnetic field, and the nonextensive distributed electrons effects. On other side, to add a valuable appreciation for the present results, let us investigate numerically the effects of different physical parameters variations; q, Γ, k, and Ω on the basic characteristics of DAWs. The plasma parameters are chosen based on typical nonthermal DP values:[9,14,16] $T_e \sim 4\,\text{eV}$, $T_i \sim 1\,\text{eV}$, $n_{i0}(0) \simeq 2 \times 10^{30}$, and $n_{e0}(0) \simeq 8 \times 10^{29}$. The equilibrium ion and electron densities are assumed to have the forms[10,18] $n_{eo}(x) = n_{eo}(0)\exp-(\alpha_e x/L)$ and $n_{io}(x) = n_{io}(0)\exp-(\alpha_i x/L)$, respectively, where L is the density scale length taken as 200. It is remarked that the equilibrium dust density, $n_{do}(x)$, is calculated from the quasineutrality equation. α_e and α_i are the density gradient scale length for electrons and ions, which can take either positive or negative values for damping or growing number densities, respectively. However, we restrict our study here to the positive values only. The plasma equilibrium number densities are plotted in Fig. 1 against x/L. It shows that all of n_{d0}, n_{e0}, and n_{i0} decrease by increasing x/L; however, the decrement of n_{d0} is more quicker than either n_{e0} or n_{i0}. Figure 2 illustrates the variation of the frequency of linear waves (real part) ω_r against x/L. In Figs. 2(a)–2(c), we find that ω_r decreases as q, Γ, and k increase though the responses of Γ, and k on ω_r is more stronger than the effect of q. The external magnetic field has a very weak effect on the DAW frequency, ω_r (not shown). Furthermore, it is obvious from these figures that there is a critical value of x/L, $(x/L)_c \simeq 1.3$, which corresponds to a minimum value of ω_r. The value of $(x/L)_c$ increases as either q, Γ, or k increases. Moreover, for $x/L < (x/L)_c$, ω_r decreases by increasing x/L, but for $x/L > (x/L)_c$, ω_r increases against x/L. A similar investigation was presented by Zhang and Xue[16] but for inhomogeneous DP model including nonthermal ions and Boltzmann electrons.

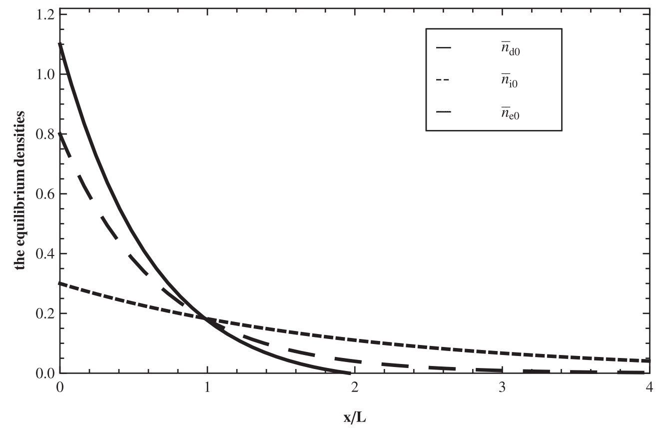

FIG. 1. The equilibrium densities versus x/L for $\delta = 2.3$, $\alpha_i = 1.5$, and $\alpha_e = 0.5$.

IV. NONLINEAR DAWS

In order to investigate the propagation of nonlinear properties of DAWs in an inhomogeneous magnetized DP, we employ the standard RPM,[10,14,16,39] and introduce the following stretching coordinate variables,

$$\zeta = \varepsilon^{1/2}\left(\int_0^x \frac{\partial x'}{\lambda_0(x')} - t\right),$$
$$X = \varepsilon^{3/2}x, \quad Y = \varepsilon^{1/2}y, \quad \text{and} \quad Z = \varepsilon^{1/2}z, \tag{8}$$

where ε measures the size of the perturbation amplitude and λ_0 is the velocity of the moving frame, to be determined later. The physical variables $n_{d,i,e}, u_{dx}, u_{dy,dz}$, and ϕ are expanded in powers of ε as

$$\left.\begin{aligned} n_{d,i,e} &= n_{d,i,e0}(X) + \varepsilon n_{d,i,e1} + \varepsilon^2 n_{d,i,e2} + \ldots, \\ u_{dx} &= u_{dx0}(X) + \varepsilon u_{dx1} + \varepsilon^2 u_{dx2} + \ldots.., \\ u_{dy,z} &= \varepsilon^{3/2} u_{dy,dz1} + \varepsilon^2 u_{dy,dz2} + \ldots..., \\ \phi &= \phi_0(X) + \varepsilon\phi_1 + \varepsilon^2\phi_2 + \ldots.., \end{aligned}\right\} \tag{9}$$

and $\Gamma = \varepsilon^{3/2} f_1$. Considering spatial gradients only leads to the relations

$$\frac{\partial n_{d,i,e0}}{\partial\zeta} = \frac{\partial\lambda_0}{\partial\zeta} = \frac{\partial u_{dx0}}{\partial\zeta} = \frac{\partial\phi_0(x)}{\partial\zeta} = 0. \tag{10}$$

At equilibrium, we find

$$\left.\begin{aligned} &\frac{\partial n_{d0}u_{dx0}}{\partial X} = 0. \\ &5\sigma\frac{\partial n_{d0}^{2/3}}{\partial X} + \frac{\partial u_{dx0}^2}{\partial X} - 2\frac{\partial\phi_0}{\partial X} + 2u_{dx0}f_1 = 0. \end{aligned}\right\} \tag{11}$$

Substituting Eqs. (8) and (9) into the basic set of Eqs. (1)–(5), and using Eqs. (10) and (11), for the lowest order equations in ε give

$$n_{d1} = -n_{d0}R\phi_1, \quad u_{dx1} = -\tilde{\lambda}R\phi_1, \quad u_{dz1} = \frac{\tilde{\lambda}^2 R}{\Omega}\frac{\partial\phi_1}{\partial Y},$$
$$u_{dy1} = -\frac{\tilde{\lambda}^2 R}{\Omega}\frac{\partial\phi_1}{\partial Z}, \tag{12}$$

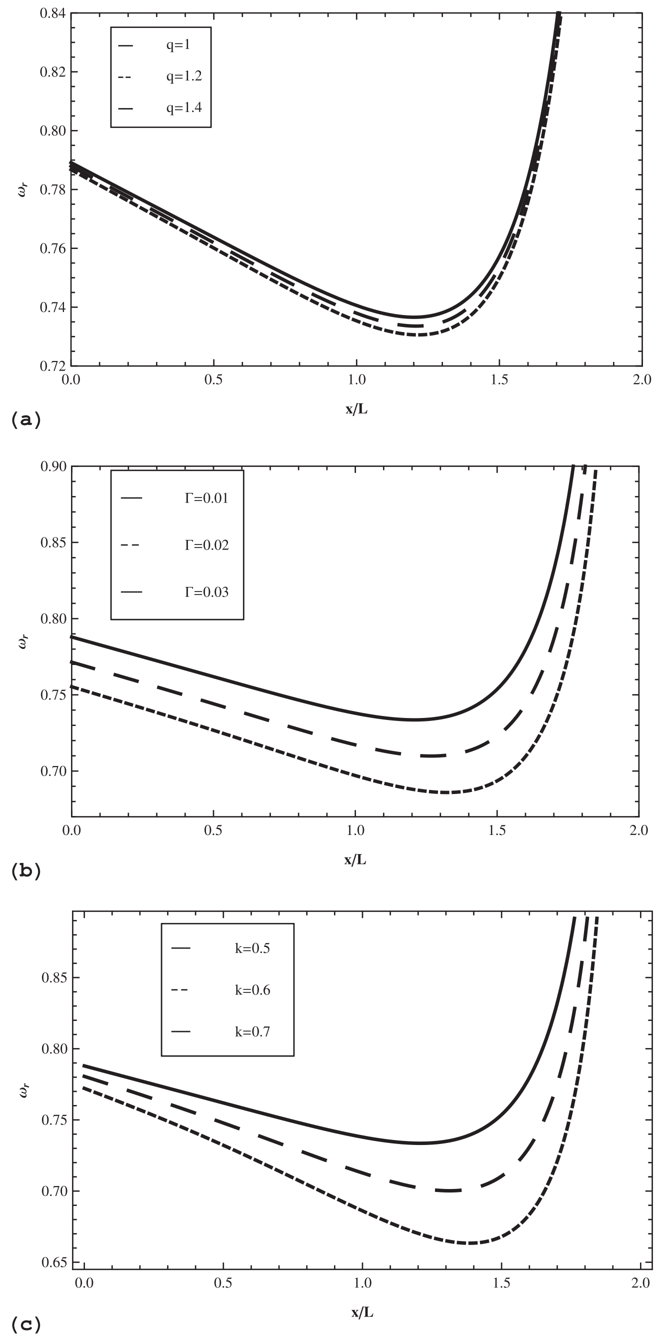

FIG. 2. Plot of ω_r against $x\,/\,L$ with different values of q, Γ, and k in panels a, b, and c, respectively, for $\sigma = 10^{-2}$, $s = 4$, $\Omega = 0.5$, $\Gamma = 0.01$, $k = 0.5$, and $k_x = 0.49$. The remaining parameters are selected as in Fig. 1.

where $R = (\tilde{\lambda}^2 - \alpha n_{d0})^{-1}$ and $\tilde{\lambda} = \lambda_0 - u_{dx0}$. λ_0 is calculated to have the form

$$\lambda_0 = u_{dx0} + \sqrt{\alpha n_{d0} + \frac{n_{d0}(\delta-1)}{\left(\frac{1+q}{2}\right) n_{e0}\left[1 - \left(\frac{q-3}{2}\right)\phi_0\right] + s\,\delta n_{i0}(1 - s\phi_0)}}. \tag{13}$$

The dependences of the velocity, λ_0 given by Eq. (13), on the variations of x/L and ϕ_0 are illustrated in Fig. 3. It shows

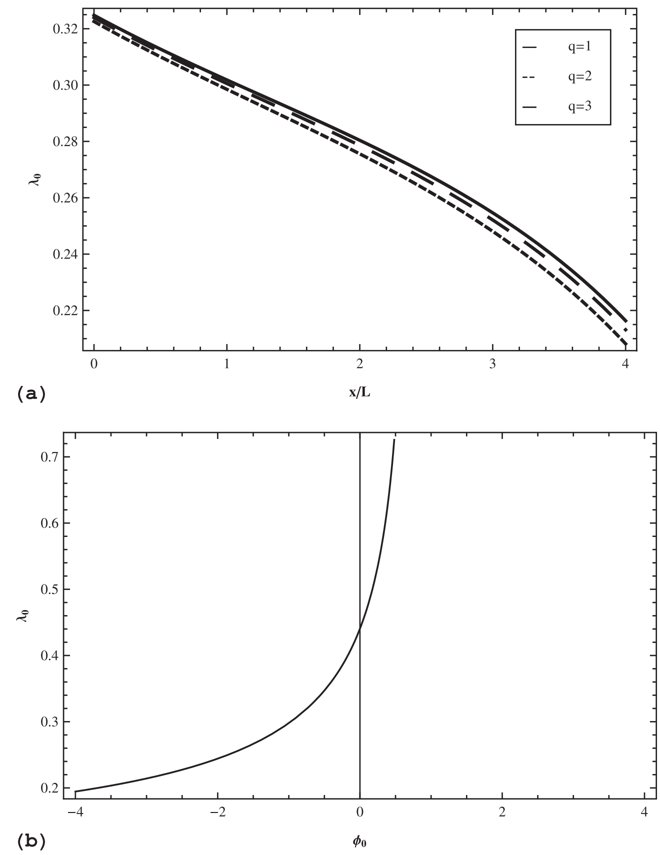

FIG. 3. Plot of λ_0 against x/L in (a) and against ϕ_0 in (b). In panel (a), $\sigma = 10^{-2}$, $s = 3$, $\delta = 3$, $\alpha_i = 0.9$, $\alpha_e = 0.5$, and $u_{dx0} = 0.02$ but in panel (b) $s = 2$, $\delta = 2$, and $x/L = 2$, the other parameters are selected as in panel (a).

that λ_0 decreases as x/L or q increases, while λ_0 increases fast due the increment in ϕ_0 where ϕ_0 has positive values. However, for negative values of ϕ_0, λ_0 is reduced by increasing ϕ_0. A similar behaviour is observed for a nonthermal inhomogeneous DP model containing nonthermal ions.[9]

Going to the next-order of ε in the perturbation theory yields to the following system of equations:

$$-\tilde{\lambda}\frac{\partial n_{d2}}{\partial \zeta} + n_{d0}\frac{\partial u_{dx2}}{\partial \zeta} + \frac{\partial (n_{d1}u_{dx1})}{\partial \zeta} + \lambda_0\left[\frac{\partial (n_{d0}u_{dx1} + n_{d1}u_{dx0})}{\partial X} + \frac{\partial n_{d0}u_{dy2}}{\partial Y} + \frac{\partial n_{d0}u_{dz2}}{\partial Z}\right] = 0, \tag{14}$$

$$-\tilde{\lambda}\frac{\partial u_{dx2}}{\partial \zeta} = u_{dx1}\frac{\partial u_{dx1}}{\partial \zeta} - \lambda_0\frac{\partial u_{dx0}u_{dx1}}{\partial X} - \alpha\frac{\partial n_{d2}}{\partial \zeta} - \alpha\lambda_0\frac{\partial n_{d1}}{\partial X} + \frac{1}{3}\alpha\lambda_0 n_{d0}^{-1} n_{d1}\frac{\partial n_{d0}}{\partial X} + \frac{1}{3}\alpha n_{d0}^{-1} n_{d1}\frac{\partial n_{d1}}{\partial \zeta} + \lambda_0\frac{\partial \phi_1}{\partial X} + \frac{\partial \phi_2}{\partial \zeta} - \lambda_0 f_1 u_{dx1}, \tag{15}$$

$$\frac{1}{\lambda_0^2}\frac{\partial^2 \phi_1}{\partial \zeta^2} + \frac{\partial^2 \phi_1}{\partial Y^2} + \frac{\partial^2 \phi_1}{\partial Z^2} = n_{d2} + \frac{1}{(\delta-1)}(n_{e2} - \delta n_{i2}), \tag{16}$$

with

$$u_{dz2} = -\frac{\tilde{\lambda}^3 R}{\Omega^2 \lambda}\frac{\partial^2 \phi_1}{\partial\zeta\partial Z}, \quad u_{dy2} = -\frac{\tilde{\lambda}^3 R}{\Omega^2 \lambda}\frac{\partial^2 \phi_1}{\partial\zeta\partial Y}. \tag{17}$$

Eliminating the second-order perturbed quantities appeared in Eqs. (14)–(16) with the help of Eqs. (12), (13), and (17), we can finally obtain the evolution equation, which has the form of a MZK equation,

$$\frac{\partial\phi_1}{\partial X} + C_1(X)\phi_1\frac{\partial\phi_1}{\partial\zeta} + C_2(X)\frac{\partial}{\partial\zeta}\left(\frac{\partial^2\phi_1}{\partial Y^2} + \frac{\partial^2\phi_1}{\partial Z^2}\right) + C_3(X)\frac{\partial^3\phi_1}{\partial\zeta^3} + C_4(X)\,\phi_1 = 0, \tag{18}$$

where

$$C_1(X) = C(X)\left\{3R^2 n_{d0}\left(\tilde{\lambda}^2 - \frac{1}{9}\alpha n_{d0}\right) - \frac{1}{R(\delta-1)}\left[\frac{1}{4}n_{e0}(q-3)(q+1) + \delta s^2 n_{i0}\right]\right\},$$

$$C_2(X) = -C(X)\left(\frac{\tilde{\lambda}^4 R n_{d0}}{\Omega^2} + \frac{1}{R}\right), \quad C_3(X) = -C(X)/(\lambda_0^2 R),$$

$$C_4(X) = -C(X)\lambda_0\left(\tilde{\lambda}\,\frac{\partial\lambda_0 R n_{d0}}{\partial X} + \tilde{\lambda}\,\frac{\partial R n_{d0} u_{dx0}}{\partial X} + n_{d0}\,\frac{\partial\tilde{\lambda} u_{dx0} R}{\partial X} + \alpha n_{d0}\frac{\partial R n_{d0}}{\partial X} - \frac{1}{3}\alpha n_{d0} R\frac{\partial n_{do}}{\partial X} + \tilde{\lambda} n_{do} R f_1\right),$$

$$C(X) = -(2\lambda_0^2\tilde{\lambda} R n_{d0})^{-1}.$$

Equation (18) describes the nonlinear propagation of the DAWs in an inhomogeneous DP systems, whose components have number density gradients with the inclusion of nonextensive electrons. It is remarked here that the coefficients $C_1(X)$ and $C_3(X)$ represent the nonlinear and the dispersion terms, however $C_4(X)$ is created due to the inclusion of the inhomogeneity and the collision effects. Figure 4 presents the variation of $C_1(X)$ as a function of x/L. It shows that for $C_1(X) > 0$ and $x/L > 1.2$ [$C_1(X) < 0$ and $0 < x/L < 1.2$], the predicted nonlinear dust acoustic solitary wave is compressive [rarefactive] soliton. For Eq. (18), by ignoring the nonthermal ion effects in the results of Ref. 9 and the nonextensive electron effects presented here, a good agreement exists.

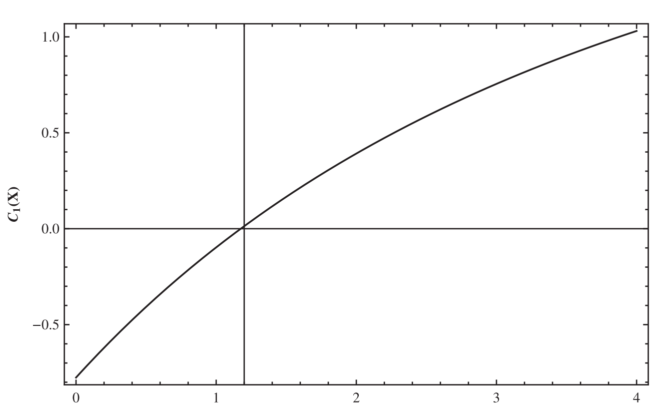

FIG. 4. Plot of $C_1(X)$ against x/L with $\sigma = 10^{-2}$, $s = 3$, $\delta = 2$, $\alpha_i = 0.3$, $\alpha_e = 0.5$, $\Omega = 0.05$, $\Gamma = 0.01$, $u_{dx0} = 0.01$, and $\phi_0 = 0.2$.

V. ANALYTICAL SOLUTION

To get the analytical solution of the derived MZK equation, Eq. (18), let us follow the transformation presented in Refs. 9 and 14

$$\phi_1(X, Y, Z, \zeta) = H(X, Y, Z, \zeta)G(X), \tag{19}$$

where $G(X)$ is the amplitude factor which is defined as

$$G(X) = \exp\left[-\int_0^X C_4(x')dx'\right] = \left(R\,\lambda\sqrt{\tilde{\lambda}\,n_{d0}}\right)^{-1}\exp\left[-\int_0^X \frac{f_1}{2\lambda}dx'\right]. \tag{20}$$

Substituting Eq. (19) into Eq. (18), we get

$$\frac{\partial H}{\partial X} + \bar{C}_1(X)H\,\frac{\partial H}{\partial\zeta} + C_2(X)\,\frac{\partial}{\partial\zeta}\left(\frac{\partial^2 H}{\partial Y^2} + \frac{\partial^2 H}{\partial Z^2}\right) + C_3(X)\frac{\partial^3 H}{\partial\zeta^3} = 0, \tag{21}$$

where $\bar{C}_1(X) = C_1(X)G(X)$.

Introducing the following parameters

$$\tau = \int^X\sqrt{\frac{\bar{C}_1^3}{C_3}}dX', \quad \eta_1 = \sqrt{\frac{\bar{C}_1}{C_3}}\zeta, \quad \eta_2 = \sqrt{\frac{\bar{C}_1}{C_2}}Y \quad \text{and} \quad \eta_3 = \sqrt{\frac{\bar{C}_1}{C_2}}Z, \tag{22}$$

into Eq. (21) yields

$$\frac{\partial H}{\partial\tau} + H\frac{\partial H}{\partial\eta_1} + \frac{\partial}{\partial\eta_1}\left(\frac{\partial^2 H}{\partial\eta_2^2} + \frac{\partial^2 H}{\partial\eta_3^2}\right) + \frac{\partial^3 H}{\partial\eta_1^3} = 0. \tag{23}$$

We define the new variable $\eta = L_x\eta_1 + L_y\eta_2 + L_z\eta_3 - V\tau$, with L_x, L_y, and L_z being the directional cosines of the wave vector along the $\zeta-$, $Y-$, and Z–axes, $L_x^2 + L_y^2 + L_z^2 = 1$ and V is the constant velocity. Using the boundary conditions; $H(\eta) \to 0, \partial H/\partial\eta \to 0, \partial^2 H/\partial\eta^2 \to 0$ as $|\eta| \to \infty$, we get the solitary solution of (23) as

$$H(\eta) = H'_m\,\mathrm{sech}^2(\eta/\mathrm{W}), \tag{24}$$

where $H'_m(=6V/L_x)$ is the amplitude and $W(=2\sqrt{L_x/V})$ is the width of the DAWs.

Now, let us return back to the original independent variables (x, y, z, and t) to express the derived solitary wave solution in terms of them. Putting the real electrostatic potential associated with the soliton solution to be $\phi \simeq \varepsilon\phi_1$ and after making some mathematical manipulation, we obtain

$$\phi(x, y, z, t) = A\,\mathrm{sech}^2(\xi/\Delta), \tag{25}$$

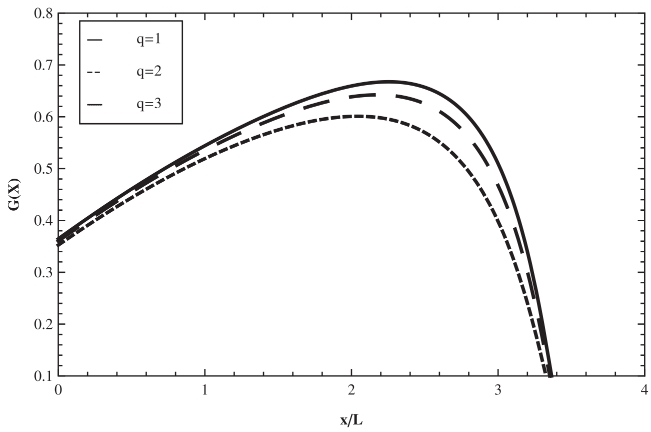

FIG. 5. Plot of $G(X)$ against x/L with $\sigma = 10^{-2}$, $s = 4$, $\delta = 2$, $\alpha_i = 0.9$, $\alpha_e = 0.3$, $\Omega = 0.5$, $\Gamma = 0.1$, $u_{dx0} = 0$, and $\phi_0 = -1$.

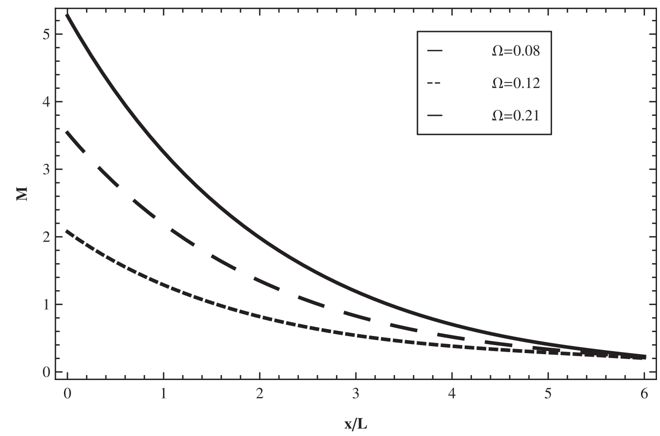

FIG. 7. Plot of Mach number M against x/L for different Ω with $\sigma = 0$, $s = 3$, $\delta = 4$, $\alpha_i = 0.9$, $\alpha_e = 0.5$, $\Gamma = 0.01$, $u_{dx0} = 0$, $q = 1$, and $\phi_0 = -1$.

where A and Δ are the amplitude and the width that are given by $A = (6V/L_x)\phi_0\tilde{\phi}$ and $\Delta = 2\sqrt{C_3(x)/(V L_x C_1(x)\phi_0\tilde{\phi})}$, respectively. ϕ_0 being the amplitude factor of the potential at $x = 0$ and $\tilde{\phi} = \tilde{\phi}(x)/\tilde{\phi}(0)$. $\xi = t - \int_0^x \frac{dx'}{M_1} - \frac{y}{M_2} - \frac{z}{M_3}$, with $M_1(x) = L_x\,\lambda_0(x)/[L_x + V\,\lambda(x)C_1(x)\phi_0\tilde{\phi}]$, $M_2(x) = (L_x/L_y)\sqrt{C_2(x)/C_3(x)}$, $M_3(x) = (L_x/L_Z)\sqrt{C_2(x)/C_3(x)}$ and $G(x) = \phi_0(0)\tilde{\phi}(x)$. Moreover, the Mach number (DAW soliton speed) is given by

$$M = \sqrt{\left(\frac{L_x\,\lambda_0(x)}{L_x + V\,\lambda_0(x)C_1(x)\phi_0\tilde{\phi}}\right)^2 + \frac{C_2(x)}{C_3(x)}\frac{L_x^2\left(1 - L_x^2\right)}{L_y^2 L_z^2}}. \tag{26}$$

Figure 5 elucidates the variation of the amplitude factor, $G(X)$ given in Eq. (20) against x/L. It is clear that there is a critical point $(x/L)_c \simeq 2.4$ at which $G(X)$ has a maximum value, this critical point moves to a smaller value of x/L by increasing the nonextensive parameter, q. $G(X)$ first increases against x/L because the inhomogeneity effect part dominates on the collision effect. Then, after $(x/L) = (x/L)_c$, $G(X)$ decreases very rapidly by increasing x/L. In the second part, for $x/L > (x/L)_c$, the inhomogeneities in the plasma components become small compared to the collision effect, which redominates again, thus $G(X)$ decreases. Finally, for larger values of x/L, $G(X)$ has very small values. On the other hand, Fig. 6 represents the behavior of the solitary wave width Δ against x/L and q. Figure 7 shows that soliton Mach number M decreases as either x/L or Ω increases. Finally, it is interesting to show the three-dimensional potential profile, ϕ, given by (25) and is released from the MZK evolution equation, (18). For this purpose, we illustrate in Fig. 8 the variations of ϕ against ξ and x/L and q. It is obvious that the soliton amplitude as well as its width increase as x/L

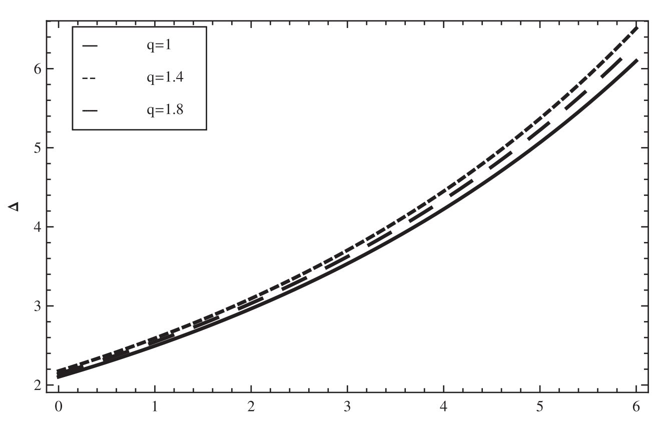

FIG. 6. Plot of the solitary width Δ against x/L for different q with $\sigma = 10^{-3}$, $s = 4$, $\delta = 3$, $\alpha_i = 0.6$, $\alpha_e = 0.5$, $\Omega = 0.5$, $\Gamma = 0.01$, $u_{dx0} = 0.2$, and $\phi_0 = 0.2$.

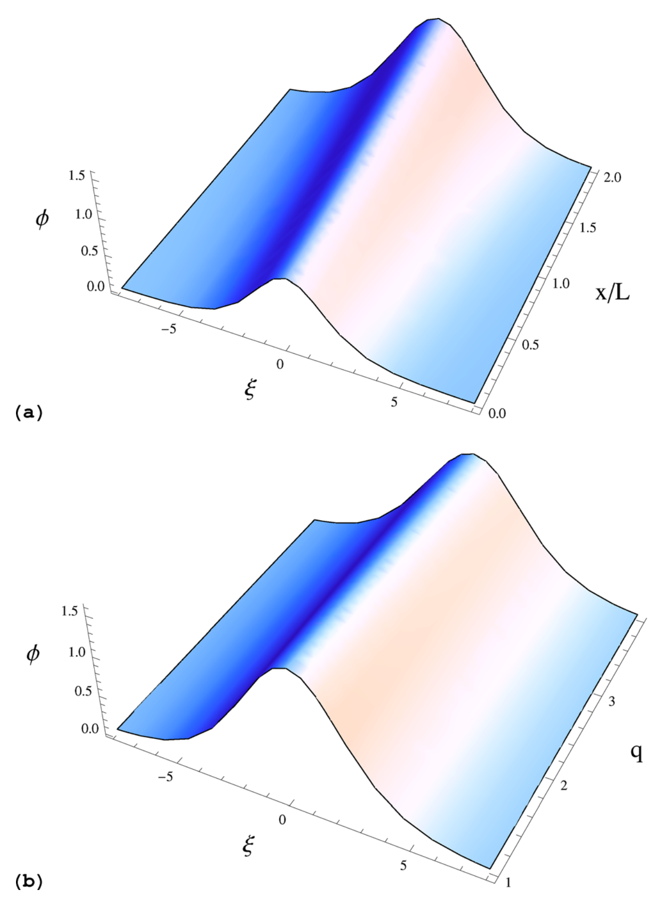

FIG. 8. The variation of the three-dimensional soliton solution, ϕ against ξ and x/L $[q]$ in (a)[(b)] with q $[x/L] = 2$, respectively. The remaining parameters are selected as in Fig. 6.

increases. However, the increment of q results as a slight reduction of the soliton amplitude with wider width. Also, from Fig. 8(a), one can observe that the soliton moves toward negative ξ direction by increasing x/L, which cannot be observed in homogeneous DP model.

VI. CONCLUSION

In summary, we have carried out both linear and nonlinear analyses of the main characteristics of the DAWs in an inhomogeneous magnetized warm DP model consisting of Boltzmann ions, nonextensive electrons, and inertial dust fluid. The standard normal mode analysis is used to derive the linear dispersion law for DAW propagation, Eq. (7). The combined effects of DP components number density inhomogeneities, nonextensive electrons, collisions and external applied magnetic field on the evolution of three dimensional nonlinear DAWs is studied in details. It is found that the DAW linear phase velocity, λ_0 decreases as the inhomogeneity parameter, x/L or the electron nonextensive parameter, q, increases. Moreover, employing a RPM, the evolution equation; variable coefficient MZK is derived. A new critical point is detected for the nonlinear coefficient around which both rarefactive and compressive DAW solitons are observed. The solution of this equation contains two part; one of them is the amplitude factor, $G(X)$, and the other is the bell-shaped sech^2-type solution. It is shown that the width of the DAW soliton increases as either q or x/L increase. However, it is seen that the external magnetic field has no effect on the DAW amplitude, its role is displayed in the decrement of the soliton speed M. The present analysis could be useful for understanding different nonlinear features of localized electrostatic disturbances in astrophysical inhomogeneous DP situations[41] or plasma experiment,[42,43] where nonextensive electrons are present.

ACKNOWLEDGMENTS

The authors would like to thank Professor Dr. S. K. El-Labany, Professor of Theoretical Plasma Physics, Faculty of Science, Damietta University for his advices, valuable suggestions and encouragements during this research work.

1E. C. Whipple, T. G. Northrop, and D. A. Mendis, J. Geophys. Res. **90**, 7405, doi:10.1029/JA090iA08p07405 (1985).
2U. de Angelis, V. Formisano, and M. Giordano, J. Plasma Phys. **40**, 399 (1988).
3C. K. Goertz, Rev. Geophys. **27**, 271, doi:10.1029/RG027i002p00271 (1989).
4J. H. Chu, J. B. Du, and I. Lin, J. Phys. D, Appl. Phys. **27**, 296 (1994).
5A. Barkan, A. R. L. Merlino, and N. D'Angelo, Phys. Plasmas. **2**, 3563 (1995).
6G. E. Morfill and H. Thomas, J. Vac. Sci. Technol. A **14**, 490 (1996).
7R. L. Merlino, A. Barkan, C. Thompson, and N. D'Angelo, Phys. Plasmas. **5**, 1607 (1998).
8N. N. Rao, P. K. Shukla, and M. Y. Yu, Planet. Space Sci. **38**, 543 (1990).
9W. F. El-Taibany, M. Wadati, and R. Sabry, Phys. Plasmas **14**, 032304 (2007).
10W. F. El-Taibany and M. Wadati, Phys. Plasmas **14**, 042302 (2007).
11W. F. El-Taibany, W. M. Moslem, M. Wadati, and P. K. Shukla, Phys. Lett. A **372**, 4067 (2008).
12S. V. Singh and N. N. Rao, Phys. Plasmas **5**, 94 (1998).
13Y.-f. Li, J. X. Ma, and D.-l. Xiao, Phys. Plasmas **11**, 5108 (2004).
14A. P. Misra and A. R. Chowdhury, Phys. Plasmas **13**, 062307 (2006).
15S. Singh and R. Bharuthram, IEEE Trans. Plasma Sci. **38**, 852 (2010).
16L. P. Zhang and J. K. Xue, Commun. Nonlinear Sci. Numer. Simulat. **15**, 3379 (2010).
17H. Alinejad and A. A. Mamun, Phys. Plasmas **18**, 073706 (2011).
18W. F. El-Taibany, Phys. Plasmas **20**, 093701 (2013).
19A. A. Samaryan, A. V. Chernyshev, O. F. Petrov, A. P. Nefedov, and V. E. Fortov, JETP **92**, 454 (2001).
20A. Rényi, Acta Math. Acad. Sci. Hung. **6**, 285 (1955).
21C. Tsallis, J. Stat. Phys. **52**, 479 (1988); C. Tsallis, *Introduction to Nonextensive Statistical Mechanics* (Springer, New York, 2009).
22A. R. Plastino and A. Plastino, Phys. Lett. A **174**, 384 (1993).
23G. Kaniadakis, A. Lavagno, and P. Quarati, Phys. Lett. B **369**, 308 (1996).
24A. Lavagno, G. Kaniadakis, M. Rego-Monteiro, P. Quarati, and C. Tsallis, Astrophys. Lett. Commun. **35**, 449 (1998).
25C. Feron and J. Hjorth, Phys. Rev. E **77**, 022106 (2008).
26A. Lavagno and D. Pigato, Eur. Phys. J. A **47**, 52 (2011).
27G. Gervino, A. Lavagno, and D. Pigato, Cent. Eur. J. Phys. **10**, 594 (2012).
28S. Abe, S. Martínez, F. Pennini, and A. Plastino, Phys. Lett. A **281**, 126 (2001).
29J. A. S. Lima, R. Silva, Jr., and J. Santos, Phys. Rev. E **61**, 3260 (2000).
30J. Du, Phys. Lett. A **329**, 262 (2004).
31M. Tribeche and A. Merriche, Phys. Plasmas **18**, 034502 (2011).
32M. Tribeche and P. K. Shukla, Phys. Plasmas **18**, 103702 (2011).
33M. Asaduzzaman, A. A. Mamun, and K. S. Ashrafi, Phys. Plasmas **18**, 113704 (2011).
34W. F. El-Taibany and M. Tribeche, Phys. Plasmas **19**, 024507 (2012).
35K. Roy, T. Saha, P. Chatterjee, and M. Tribeche, Phys. Plasmas **19**, 042113 (2012).
36A. S. Bains, M. Tribeche, and C. S. Ng, Astrophys. Space Sci. **343**, 621 (2013).
37S. Ashraf, S. Yasmin, M. Asaduzzaman, and A. A. Mamun, Astrophys. Space Sci. **348**, 495 (2013).
38N. Akhtar, W. F. El-Taibany, and S. Mahmood, Phys. Lett. A **377**, 1282 (2013).
39T. Taniuti and C. C. Wei, J. Phys. Soc. Jpn. **24**, 941 (1968); N. Asano and T. Taniuti, *ibid.* **27**, 1059 (1969); N. Asano and H. Ono, *ibid.* **31**, 1830 (1971).
40S. K. El-Labany, W. F. El-Taibany, and O. M. El-Abbasy, Phys. Plasmas **12**, 092304 (2005).
41J. Gong and J. Du, Phys. Plasmas **19**, 063703 (2012).
42J. M. Liu, J. S. De Groot, J. P. Matte, T. W. Johnston, and R. P. Drake, Phys. Rev. Lett. **72**, 2717 (1994).
43C. Yin and J. Du, Physica A **407**, 119 (2014).